Korean J. Chem. Eng., **25**(6), 1300-1308 (2008)

Effect of dissolved oxygen concentration and light intensity on photocatalytic degradation of phenol

M. Subramanian and Aravamudan Kannan†

Department of Chemical Engineering, Indian Institute of Technology Madras, Chennai, Tamil Nadu 600 036, India
(*Received 14 March 2008 • accepted 3 May 2008*)

Abstract−Catalyst loading is an important parameter that needs to be optimized in the operation of photocatalytic slurry reactors. In this study on photocatalytic degradation of phenol, the optimum catalyst loading was found to depend mainly on the dissolved oxygen (DO) concentration in the aqueous solution, especially at higher irradiation intensities. The estimated Langmuir-Hinshelwood (L-H) kinetics constants were found to vary with light intensity and dissolved oxygen concentration. The intermediate products of photocatalytic oxidation were identified.

Key words: Photocatalysis, Optimum Catalyst Loading, Slurry Reactor, Langmuir-Hinshelwood Kinetics, Intermediates

INTRODUCTION

Photocatalysis is an advanced oxidation process that is receiving widespread attention as it has the potential to mineralize toxic organic contaminants in water and air [1]. It is essential to understand the contributions of several factors influencing the intrinsic kinetics of pollutant degradation from batch reactor studies. The major reactions taking place in the presence of the TiO_2 photocatalyst and UV radiation are given below [2-4].

$$TiO_2+h\nu \rightarrow h^+ + e^- \quad (1)$$

$$h^+ + OH^- \text{ (or } H_2O) \rightarrow {}^{s}OH \quad (2)$$

$$e^- + O_2 \rightarrow {}^{s}O_2^- \quad (3)$$

$$\text{Organics} + {}^{s}OH \rightarrow \text{intermediates} \rightarrow CO_2 + H_2O + \text{mineral acids} \quad (4)$$

Reaction (1) occurs by illuminating the TiO_2 particles with ultraviolet irradiation of wavelengths shorter than 387 nm. This reaction, involving the generation of holes (h^+) and electrons (e^-), is central to the efficacy of the oxidation process. The rate of this reaction depends on the light intensity and the catalyst concentration. The degradation and eventual mineralization of the pollutants (reaction 4) is mainly determined by the concentration of hydroxyl radicals (^{s}OH). The concentration of holes and their reaction with the hydroxyl ion (or water) determines the ^{s}OH concentration as shown in reaction 2. However, some of the holes may also be consumed by free electrons leading to their reduced availability for the hydroxyl radical production. The dissolved oxygen in the reaction mixture acts as a scavenger of electrons (reaction 3), thereby reducing the rate of electron-hole recombination.

From the above discussion, in addition to light intensity and catalyst loading, the dissolved oxygen (DO) concentration also may play an important role. Quantifying the effects of all these variables will help in the design and operation of the photocatalytic reactor. According to reaction (1), if the photocatalyst loading is low, the rate of hole generation will be low even at high light intensities. The incident light will be simply transmitted through the photocatalytic reactor. At increased catalyst loadings however, there would be absorption and scattering effects, which limit light penetration into the bulk of the reactor. In addition, there will be a greater tendency for electron-hole recombination. The dissolved oxygen concentration levels are also important as they determine the rate of scavenging of electrons. For reactors operated at low light intensities, the limiting factor is more likely to be the availability of photons and consequently holes rather than the catalyst loading and DO concentrations. A brief summary of the work reported in the literature on the effect of the various parameters on batch reaction kinetics is given below.

Peral et al. [5] observed improved yields of phenol degradation with ZnO catalyst at higher DO concentrations. Augugliaro et al. [2] reported that the kinetic constants of nitrophenol degradation at low partial pressures of oxygen were enhanced with the increasing concentration of oxygen. Terzian and Serpone [6] reported that the conversion of xylenol was sufficiently improved with oxygen-saturated suspensions when compared to air-saturated suspensions. Ilisz et al. [7] observed that below the saturation concentration of DO, initial rate of phenol degradation increased with increase in DO concentration. Almquist and Biswas [8] observed that at high concentrations of pollutant of the order of DO concentration or higher, the efficiency of photo-degradation increased with increasing DO concentration. These studies show that the DO concentration is an important factor affecting the photo-degradation kinetics. The improvement in reaction rates at high concentrations of DO has been attributed to the high surface coverage of oxygen on the catalyst and the electron scavenging effect.

Wang et al. [9] observed that at high concentrations of organic pollutants and high intensity UV irradiation, the rate of hole-initiated reactions would be fast. However, it would be also limited by the rate of electron scavenging by dissolved oxygen. When the electron scavenging effect is not sufficiently fast, excess electrons will accumulate on the TiO_2 particles causing the undesired electron-hole recombination. Stafford et al. [10] found that at high irradiation intensities, initial rate of dissolved oxygen consumption increases linearly with increase in TiO_2 concentration. Hirakawa et al. [11] have experimentally shown that the rate of decrease in concentration of dis-

†To whom correspondence should be addressed.
E-mail: kannan@iitm.ac.in

solved oxygen increased with increase in light intensity. These studies show that the dissolved oxygen concentration is related to catalyst loading and light intensity.

In the literature [12-14] mainly light transmission limitations into the slurry were attributed to the poor performance of the reactor beyond certain catalyst loadings. However, at high light intensities, DO concentration may also set a limit on the optimum catalyst loading and hence the performance of the reactor. To our knowledge, there have been no studies available to show the concomitant effects of light intensity and dissolved oxygen concentration on the optimal catalyst loading. Hence, experiments have been carried out at different dissolved oxygen concentrations, catalyst loadings and light intensities. The effects of these parameters in determining the optimum conditions of a batch photocatalytic reactor are discussed in detail. Phenol was chosen as the model compound as it is a common pollutant in industrial wastewater. It is also a suitable compound to understand and quantify the factors affecting the design of a photocatalytic reactor [15].

EXPERIMENTAL

1. Materials

Phenol and other chemicals needed for quantifying intermediates (catechol, hydroquinone, p-benzoquinone, resorcinol) were of AR grade and procured from Ranbaxy Laboratories Ltd., India. Distilled water was used in the reactions and Millipore™ water was used for analytical purposes. Two different lamps of 125 W and 6 W (Philips™ UV-A) were used as the source of ultraviolet radiation. Industrial grade air and oxygen were used in the reactions. P25 TiO_2 supplied by Degussa India Pvt Ltd., Mumbai, was used as the catalyst. A 20 kHz ultrasonic bath (Toshniwal Process Instruments Pvt. Ltd., India) was used in preparation of TiO_2 slurry.

2. Reactor Details

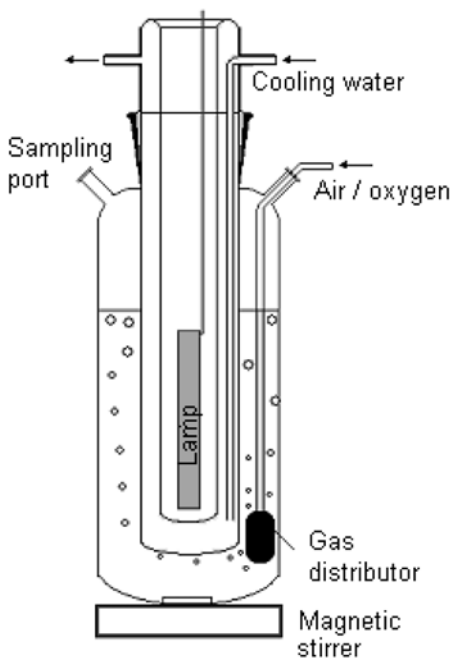

Fig. 1. Schematic of immersion-well batch reactor.

The immersion-well batch reactor, shown in Fig. 1, was comprised of a jacketed borosilicate immersion well (outer diameter: 38 mm) housed within an outer borosilicate cylinder (inner diameter: 67 mm). This assembly was placed over a magnetic stirrer. The electrical unit with an inbuilt capacitor-ballast arrangement, provided fluctuation free power input to the lamp. Water was circulated through the jacket of the immersion-well to remove the heat generated from the lamp, and to maintain the reaction temperature constant at 30±1 °C. Air or oxygen was bubbled at the desired flow rates through the reaction mixture with the help of a porous distributor.

3. Experimental Procedures

Catalyst slurry of known TiO_2 loading was prepared by using distilled water. This slurry was sonicated for 15 minutes in an ultrasonic bath to ensure uniform catalyst dispersion. Phenol stock solution was added to the slurry in sufficient amounts to get the required concentration of the pollutant. This mixture was stirred in the dark for 30 minutes with a magnetic stirrer for attaining adsorption equilibrium [16]. Phenol concentration of the slurry at the end of this period is taken as the initial value (C_0). The feed slurry was maintained at natural pH conditions (pH=6.8). DO of this normal feed slurry was measured to be 6.4 mg/L. For pre-saturating the feed with oxygen, the gas was bubbled at 300 mL/min through the slurry for about 15 minutes. Unless otherwise stated, the feed slurry was not pre-saturated. 310 mL of the slurry was charged into the illuminated reactor. Magnetic stirring and either air or oxygen supply were simultaneously turned on. The samples (approx 1-2 mL) were filtered through a 0.45 mm syringe filter, and stored in the dark for further analysis.

4. Analytical Methods

Jasco® HPLC with C18 column and photodiode array detector was used for measuring the concentrations of phenol and the intermediates formed during photocatalysis. The solvent used was acetonitrile-water (35 : 65, v/v) at a flow rate of 1 mL/min [17]. The dissolved oxygen concentration was measured by the Winkler chemical method [18]. Intensity of light received by the reactor was measured with potassium ferrioxalate actinometry [19]. The light intensity was estimated to be 1.55×10^{-4} and 50.9×10^{-4} Einstein/L·min for the 6 and 125 W lamps, respectively. Light flux (W/m^2) at the outer surface of the reactor was measured with a Lutron UV-340 radiometer.

RESULTS AND DISCUSSION

The initial nominal concentrations of phenol were usually 50 mg/L when the 125 W lamp was used. However, when the 6 W lamp was used, the initial concentration was fixed at 20 mg/L so that sufficient degradation of phenol could be ensured within a reasonable period of time (typically 1-1.5 hours). Aeration/oxygenation flow rates were set usually at 100 mL/min. Reproducibility of the experimental results was found to be within ±2%.

1. Light Transmittance Versus Catalyst Loading

Light transmittance at the outer walls of the reactor was measured with the Lutron radiometer. Oxygen gas was bubbled through the reaction mixture to replicate actual operating conditions. Fig. 2 shows the light transmittance (I'/I_o) versus catalyst loading for the lamps 6 W and 125 W. I_o refers to the light flux in W/m^2 measured

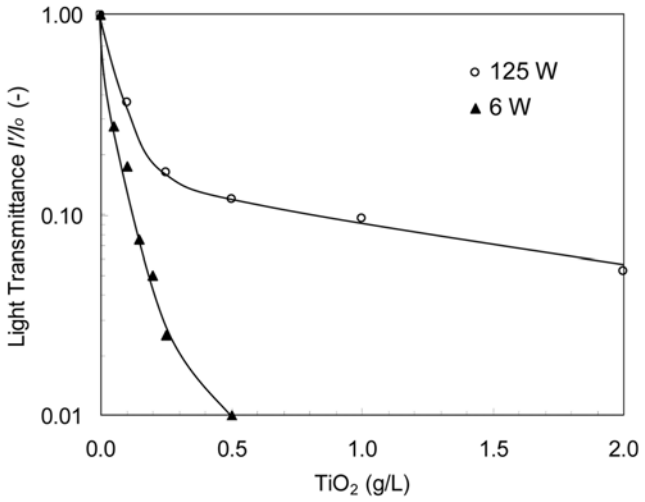

Fig. 2. Light transmittance at the outer surface of immersion-well batch reactor.

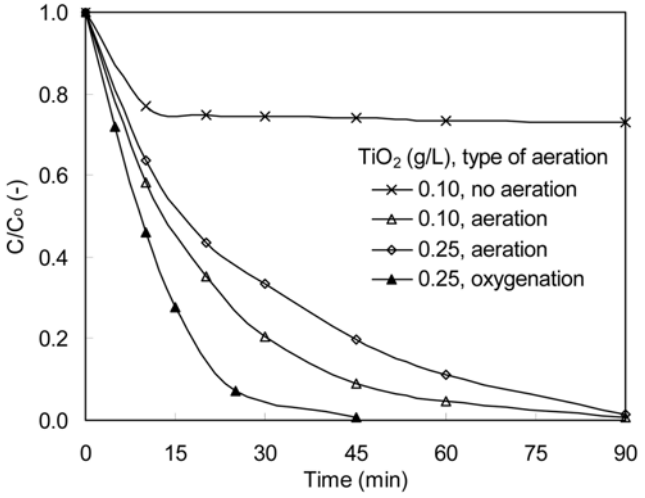

Fig. 4. Effect of gas addition on phenol degradation (125 W, C_o= 50 ppm phenol).

at the outer cylinder surface of the reactor, when the reactor is not loaded with the catalyst. I′ refers to the light flux at a given catalyst loading. This figure shows that for 6 W, light transmittance is almost nonexistent at catalyst loadings higher than 0.5 g/L. For 125 W, light transmittance is still not attenuated even after a catalyst loading of 1.0 g/L. This shows that if light transmission is the factor deciding the optimum catalyst loading, 0.5 g/L of TiO_2 would be the optimum value with 6 W and 1 g/L (or slightly higher) would be the desired loading for 125 W. Hence, the apparent optimum catalyst loading increases with increase in intensity of light used.

2. Effect of Catalyst Loading at High Irradiation Intensities (125 W)

Effect of catalyst loading on initial rate of phenol disappearance under normal operating conditions (i.e., without oxygen presaturation of the feed) is shown in Fig. 3. From this figure, it may be seen that the optimum catalyst loading corresponds to 0.1 g/L with aeration and 0.25 g/L with oxygenation. Experiments performed at different gas flow rates (0-300 mL/min) at these optimum catalyst loadings indicated that there was no significant improvement in degradation rates after 100 mL/min. Phenol conversions at the optimal catalyst loadings are reported in Fig. 4. With pure oxygen addition, degradation was 99% complete in 45 minutes as against 90 minutes with air addition. With no gas addition during the reaction, the progress of the reaction was negligible after about 10 minutes. This shows that either aeration or oxygenation is essential for sustaining the reaction progress. Oxygenation is more effective when compared to that of aeration.

If light penetration through the reactor is the only factor deciding the catalyst loading, then it appears that a loading of 1 g/L or even higher is allowable according to the discussion in the previous section. However, our results show a lower optimum loading and again it varies with the nature of gas added. Hence, other parameters also influence the degradation kinetics and these must be taken into consideration. This effect was further analyzed by measuring the dissolved oxygen concentration during the course of reaction.

3. Effect of Mode of Gas Addition at High Irradiation Intensities (125 W)

In most continuous reactor studies, either an oxygen-saturated feed (with no further aeration/oxygenation) or an oxygen unsaturated feed with continuous supply air/oxygen during the course of the reactions is used. To understand the significance of oxygen presence during the course of the reactions, four different strategies as

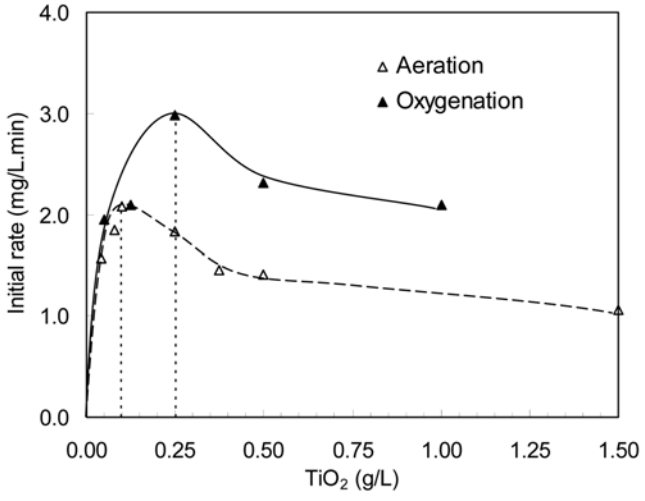

Fig. 3. Initial rate of phenol degradation versus catalyst loading for 125 W lamp (optimum catalyst loadings for air and oxygen are indicated by the vertical dashed lines).

Table 1. Different strategy of experiments with 125 W lamp

Strategy	Pre saturation of feed slurry with oxygen	Air or oxygen addition to the slurry during reaction
A	X	X
B	X	√
C	√	X
D	√	√

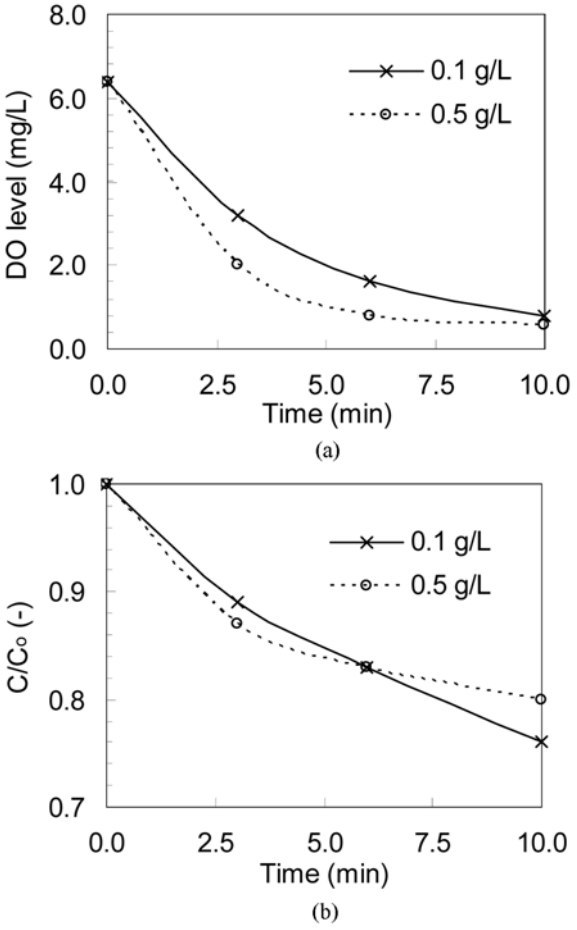

Fig. 5. (a) Dissolved oxygen concentration as a function of TiO_2 loading when no gas is added to the reaction mixture. Lamp power rating is 125 W for these conditions. (b) Phenol degradation as a function of TiO_2 loading, when no gas is added to the reaction mixture. Lamp power rating is 125 W for these conditions.

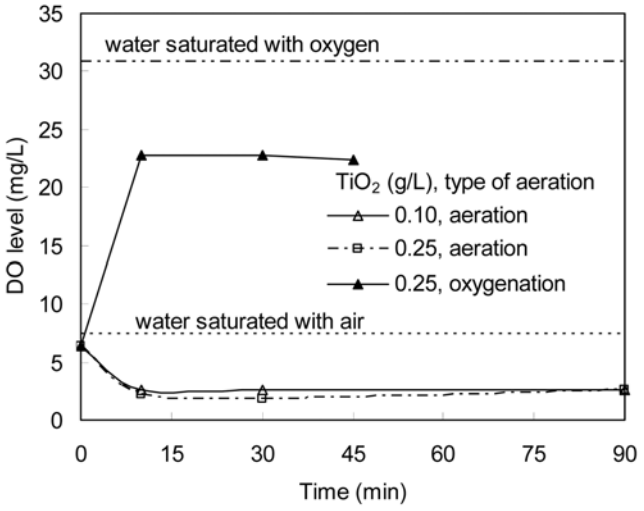

Fig. 6. Dissolved oxygen (DO) concentration in the reactor when either oxygen or air was added continuously. No presaturation of the feed with oxygen was carried out. Lamp power rating is 125 W for these conditions.

categorized in Table 1 were adopted. The effects of these strategies are discussed next.

3-1. Normal Feed Slurry without Subsequent Oxygen/Air Addition (Strategy A)

The decrease in DO during the course of reaction was monitored at different catalyst loadings (Fig. 5a). DO reduction and initial rate of photocatalytic reaction was faster at 0.5 g/L catalyst loading than at 0.1 g/L (Fig. 5b). For a given initial DO level and light intensity, the higher the TiO_2 concentration, the higher is the rate of production of holes and electrons. This leads to a higher initial rate of reaction but simultaneous faster utilization of dissolved oxygen. Hence, after a few minutes of reaction, the reaction mixture is starved of oxygen and conversion becomes actually *lower* at higher photocatalyst loadings due to electron hole recombinations.

3-2. Bubbling Air/Oxygen During the Course of Reaction into the Normal Feed Solution (Strategy B)

The variations in the DO levels are shown in Fig. 6. With aeration, the DO concentration reduced rapidly and remained at 2.6 mg/L for 0.1 g/L TiO_2 and at about 2.0 mg/L for 0.25 g/L TiO_2. When pure oxygen was added, the DO level increased rapidly and remained at 22.4 mg/L until the end of the reaction. Bubbling pure oxygen rather than air ensures a higher concentration of oxygen in the aqueous slurry. The effect of gas addition and catalyst loadings on the phenol degradation patterns was already illustrated in Fig. 4.

3-3. Pre-saturation of Slurry with Oxygen without Subsequent Aeration/Oxygenation (Strategy C)

Conversions obtained under these conditions were compared with those from unsaturated feeds (strategy A) in Fig. 7a. It may be seen that the pre-saturated feed enabled higher conversions. This may be attributed to the higher amount of initial DO present. However, the progress of reactions slowed down after certain time. This slowdown may be attributed to the decrease in dissolved oxygen levels from an initial value of 6.4 mg/L for the unsaturated feed and 27 mg/L for the pre saturated feed to a final value around 0.5 mg/L.

3-4. Pre-saturating the Feed with Oxygen and Subsequently Adding Air/Oxygen to the Reacting Slurry (Strategy D)

Pre-saturating of the feed with oxygen enabled higher initial rates when compared to the unsaturated feed (Fig. 7b, 7c). This may be attributed to the higher amount of initial DO present. After some time, the rate from strategy D was initially comparable and subsequently *even lower* when compared to strategy B where the feed slurry was not pre-saturated. Faster initial reaction rates in strategy D produced higher amounts of intermediates, such as p-benzoquinone, which also compete along with phenol for the available hydroxyl radicals.

These studies clearly show that continuous addition of air or oxygen to the reaction mixture is required to sustain the photocatalytic reaction and to effect complete conversion. Pre-saturation alone enables higher degradation rates but for a limited period only. Without subsequent addition of air/oxygen, the reaction rate is slow as the rate of DO addition by surface aeration is less than what is required by the reaction. The results indicate that for faster mineralization of the primary pollutant, strategy B is better than that of D.

At high catalyst loadings, higher numbers of electrons will accompany the higher rate of generation of holes. To minimize elec-

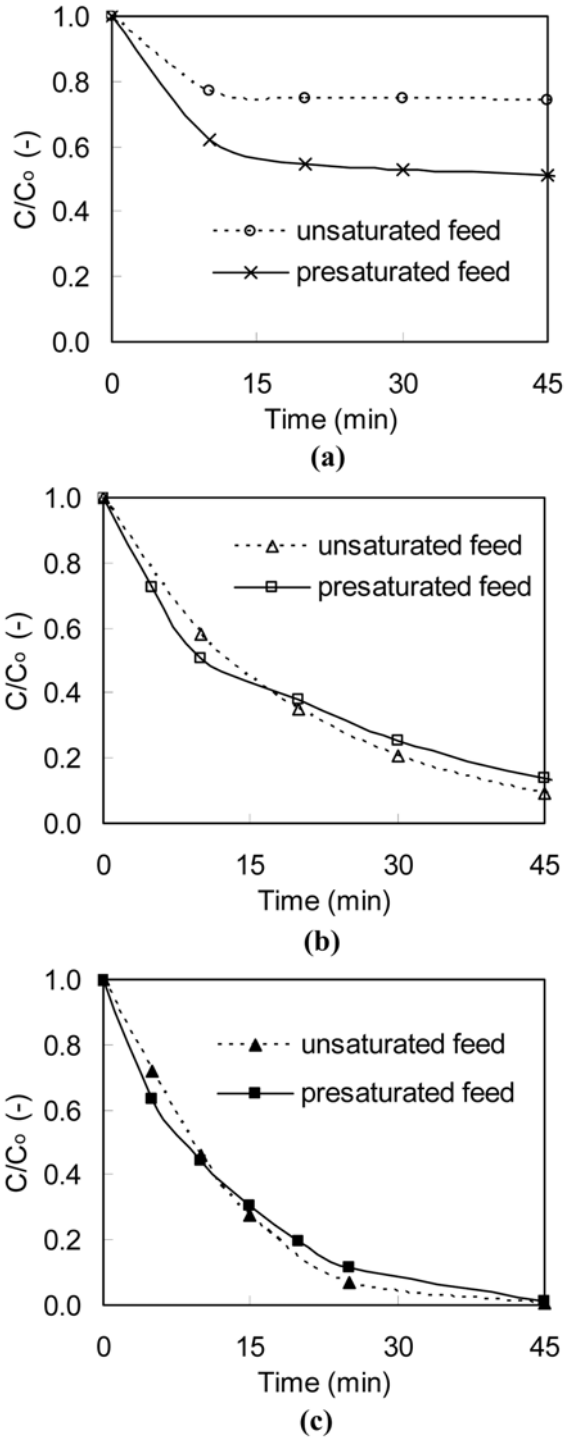

Fig. 7. Degradation of pre-saturated and normal feed solutions of phenol with 125 W lamp (full lines represent the pre-saturated feeds and dashed lines represent the normal feed): (a) no aeration, 0.1 g/L TiO_2, (b) aeration, 0.1 g/L TiO_2, (c) oxygenation, 0.25 g/L TiO_2.

tron-hole recombination, higher amounts of dissolved oxygen levels are also required. Hence, at catalyst loading higher than the optimum (0.1 g/L), the rate limitation is by insufficient amount of dissolved oxygen when aeration is the route for oxygen supply. However, in the presence of oxygenation, the residual levels of DO are maintained at high values (22.4 mg/L). Hence, the fall in reaction rates at higher than optimum catalyst loadings (>0.25 g/L) may now be attributed to the shielding effect of the TiO_2 particles. Thus, a limitation due to shielding occurs at much higher catalyst loadings when oxygen is not a limiting factor in the reactor. At high irradiation intensities, two factors may be identified to cause the rate limitation. One factor is due to inadequate availability of holes. This may arise due to low light intensity, low catalyst loadings and/or inadequate levels of DO to minimize electron-hole recombination. The second factor is the shielding effect of the TiO_2 particles. Only at higher catalyst loadings does the shielding effect become important. For instance, aeration led to an optimal catalyst loading of only 0.1 g/L due to mainly DO limitations. When DO supply was ensured by oxygenation, the shielding effects became limiting only at 0.25 g/L of catalyst loading, i.e., an increase by 2.5 times. However, this is still lower than the loading suggested from radiometry measurements, which implies that the actual reaction rates are better indicators of the optimal catalyst loadings rather than light intensity measurements carried out at the outer walls of the reactor.

When aeration is used for economic reasons to supply oxygen, the fall in reaction rate should not be wrongly attributed to the catalyst shielding effect inside the reactor. The improvements achieved due to higher catalyst loadings possible in oxygen-rich environment are quantified in Table 2 in terms of the Langmuir-Hinshelwood rate constants that will be explained in section 6.

4. Catalyst loading at low irradiation intensities (6 W)

The minimum catalyst loading for ensuring maximum rates of degradation was observed to be approximately 0.5 g/L irrespective of whether air or oxygen was added (Fig. 8). The nature of these curves is different when compared to that of 125 W irradiation (Fig. 3). From 0.1 to 0.5 g/L catalyst loading, the initial reaction rate increased slowly. Beyond this value, the initial rates were almost constant. However, with 125 W irradiation, the initial rates versus catalyst loading showed a distinct maximum.

The light intensity per unit area of the immersion well was estimated to be 0.42×10^{-6} Einstein/cm^2·min. This value is comparable to photocatalysis experiments carried out with solar irradiation. At low light intensities comparable to the UV intensity of sun (~0.2×10^{-6} Einstein/cm^2·min), uptake of oxygen by the liquid from the atmosphere is sufficient for the removal of electrons [20]. Hence, at low irradiation levels dissolved oxygen levels may not be the limiting factor in determining the rate of reaction and maximum catalyst loading.

5. Effect of Gas Addition on the DO Levels in the Reacting Mixture (6 W)

The conversion during the conditions of air, oxygen or no gas addition conditions with the normal feed (i.e., oxygen unsaturated feed) are compared in Fig. 9. The corresponding DO levels are shown in Fig. 10. In the absence of gas addition, DO levels were observed to decrease with reaction time. However, this rate of decrease was much slower when compared to that of the 125 W irradiation case (Fig. 5a). This may be attributed to the lower rate of generation of holes and electrons at lower light intensities. Hence, the demand on the available DO was lower.

With air/oxygen addition, the DO concentration in the slurry increased from the initial value of 6.4 mg/L and tended towards the respective saturation values during the course of the reaction. How-

Table 2. Experimental conditions and Langmuir-Hinshelwood kinetic constants (Optimal catalyst loadings at different aeration and light intensity conditions are shown in bold)

S. No	Lamp power rating (Watt)	Type of aeration	TiO_2 loading (g/L)	k (mg/L·min)	K (L/mg)	Initial rate (mg/L·min)	Overall quantum yield $\times 10^2$
1	125	air	0.04	2.63	0.040	1.54	0.32
2	125	air	**0.1**	2.94	0.039	2.09	0.44
3	125	air	0.5	2.13	0.042	1.41	0.29
4	125	oxygen	**0.25**	5.41	0.038	3.00	0.63
5	6	air	0.04	0.34	0.070	0.24	1.65
6	6	air	0.1	0.41	0.065	0.34	2.33
7	6	air	**0.5**	0.42	0.086	0.35	2.40
8	6	oxygen	**0.5**	0.57	0.052	0.47	3.23

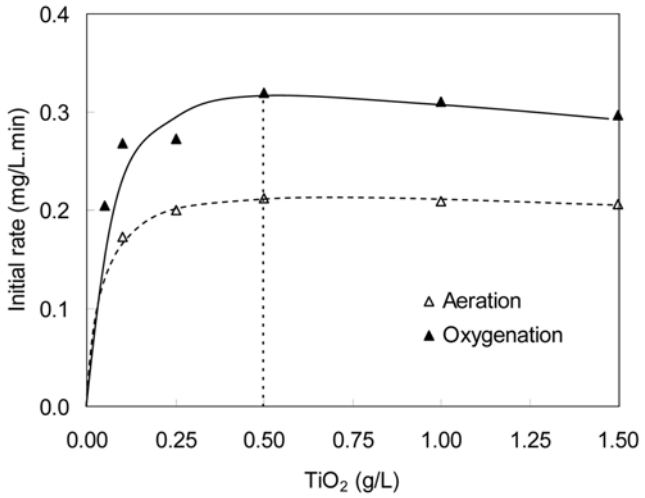

Fig. 8. Initial rate of phenol degradation versus catalyst loading for 6 W lamp (optimum catalyst loadings for aeration and oxygenation are indicated by the vertical dashed lines).

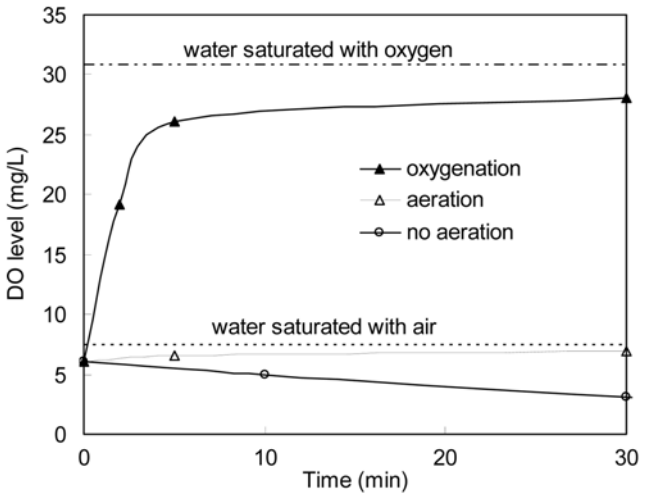

Fig. 10. Dissolved oxygen (DO) concentration in the reactor when either oxygen or air was added continuously. No presaturation of the feed with oxygen was carried out. Lamp power rating is 6 W for these conditions.

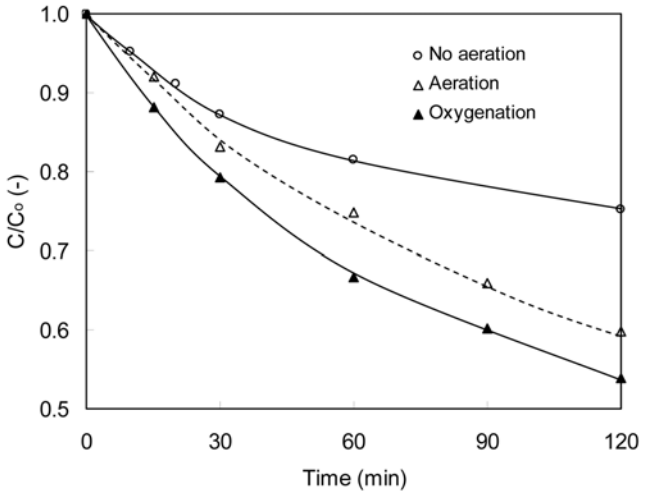

Fig. 9. Effect of gas addition on phenol degradation with 6 W lamp (C_o=50 ppm phenol, 0.5 g/L TiO_2).

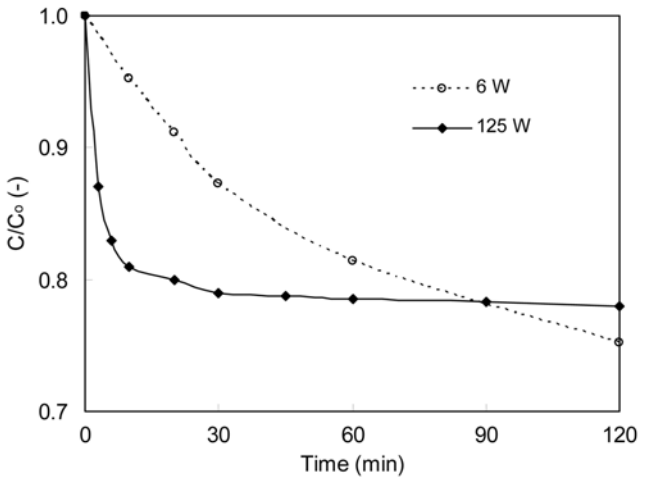

Fig. 11. Phenol degradation as a function of lamp power rating, when no gas is added to the reaction mixture. Catalyst loading is 0.5 g/L for these conditions.

ever, in the 125 W lamp case, the DO level actually decreased with aeration and tended towards sub-saturation limits with oxygenation as was shown previously in Fig. 6.

The conversion of phenol in an unsaturated feed and without any

subsequent gas additions is compared at different lamp intensities in Fig. 11. With 125 W irradiation the reaction progress was almost curtailed after the initial period, whereas with 6 W irradiation, the reaction continued to progress. Hence, at low light intensities dissolved oxygen concentration may not be the limiting factor. However, air/oxygen addition improves the reaction rate maintaining the oxygen levels required for scavenging the electrons.

6. Langmuir-Hinshelwood Kinetics Modeling

It is important to relate the reaction kinetics parameters to the light intensity, catalyst loading and DO concentration. The Langmuir-Hinshelwood (L-H) kinetics form is commonly adopted in photocatalysis literature for modeling the initial reaction rates [12,21,22].

6-1. Estimating L-H Constants

The rate of degradation of organic compounds under constant surface coverage of oxygen maybe expressed as

$$-r = k\Theta \tag{5}$$

where the apparent kinetic constant $k=k_1\Theta_{O_2}$. Here Θ is the fractional site coverage of the reactant on the catalyst surface, and a is the fractional site coverage of oxygen on the catalyst surface.

Using the Langmuir adsorption isotherm, Θ may be expressed as follows:

$$\Theta = \frac{KC}{1+KC+\sum_{i=1}^{N} K_i E_i} \tag{6}$$

where K is the apparent adsorption equilibrium constant for the primary organic pollutant (here, phenol) and C is its concentration. K_is refers to apparent adsorption equilibrium constants for the intermediate species formed during the course of photocatalytic degradation and E_is refer to their concentration.

Initially, the concentrations of the intermediates would be negligible and Eq. (6) simplifies to

$$\Theta = \frac{KC_o}{1+KC_o} \tag{7}$$

Hence, Eq. (7) may be written for initial reaction rate ($-r_o$) as

$$-r_o = \frac{kKC_o}{1+KC_o} \tag{8}$$

The constants (k and K) of this model equation maybe obtained from the initial rate kinetics by taking the reciprocal of the above equation as:

$$\frac{1}{-r_o} = \frac{1}{kKC_o}\frac{1}{} + \frac{1}{k} \tag{9}$$

The phenol degradation rates at different initial phenol concentrations encompassing the nominal value (C_o) investigated in this work were measured. With 125 W, the initial concentration was varied in the range 20-120 ppm; and with 6 W, the initial concentration was varied in the range 10-50 ppm. From initial rate measurements, the constants of Langmuir-Hinshelwood model, k (the apparent kinetic constant) and K (the apparent adsorption equilibrium constant) were obtained by fitting (with R^2 of 0.9) the initial rate experiment data ($-1/r_o$) vs. ($1/C_o$) as shown in Fig. 12. The L-H constants are shown in Table 2.

6-2. Predicting the Overall Degradation Pattern with L-H Constants Estimated from Initial Rates

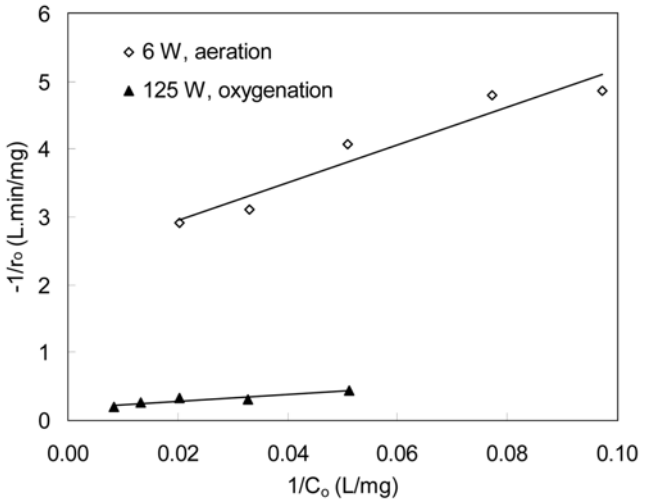

Fig. 12. Estimating Langmuir-Hinshelwood model parameters (6 W, 125 W).

The contribution from the intermediates in Eq. (6) may be accounted for in the following manner [2,22-24]

$$KC + \sum K_i E_i \approx KC_o \tag{10}$$

Hence, Eq. (8) maybe written for the entire course of reaction as

$$-r = \frac{kKC}{1+KC_o} \tag{11}$$

Integrating Eq. (11) we get,

$$C = C_o \exp\left(\frac{-kK}{1+KC_o}t\right) \tag{12}$$

The concentrations predicted from Eq. (12) were compared to the experimental data as shown in Fig. 13a, b. This prediction was found to reasonably match with the experimental data for the initial period of degradation (until about 50% conversion of the parent pollutant). Later, the discrepancies between the predictions and experimental data were found to be within ±20%.

6-3. Effect of Dissolved Oxygen Concentration, Light Intensity and Catalyst Loading on L-H Constants

The L-H constants and initial reaction rates at various experimental conditions are summarized in Table 2. The presence of oxygen increases the apparent kinetic constant k. This may be attributed to higher coverage of the catalyst surface with oxygen molecules, which increases the lifetime of the hole thereby increasing the concentration of hydroxyl radicals. Chorr et al. [25] earlier observed that photo-degradation of phenol was strongly affected by adsorbed oxygen concentration.

It was observed that at a given catalyst loading and aeration type, the apparent kinetic constant (k) varied directly with light intensity while the apparent adsorption equilibrium constant (K) was seen to have the opposite trend. These trends are consistent with the earlier observations of Emeline et al. [26] Xu and Langford [27]. For degradation of phenol with Aldrich™ TiO_2 catalyst, data of Ilisz et al. [7] and Sobczynski et al. [28] also agree with this trend.

Using a pseudo-steady state approach, Ollis [29] has explained

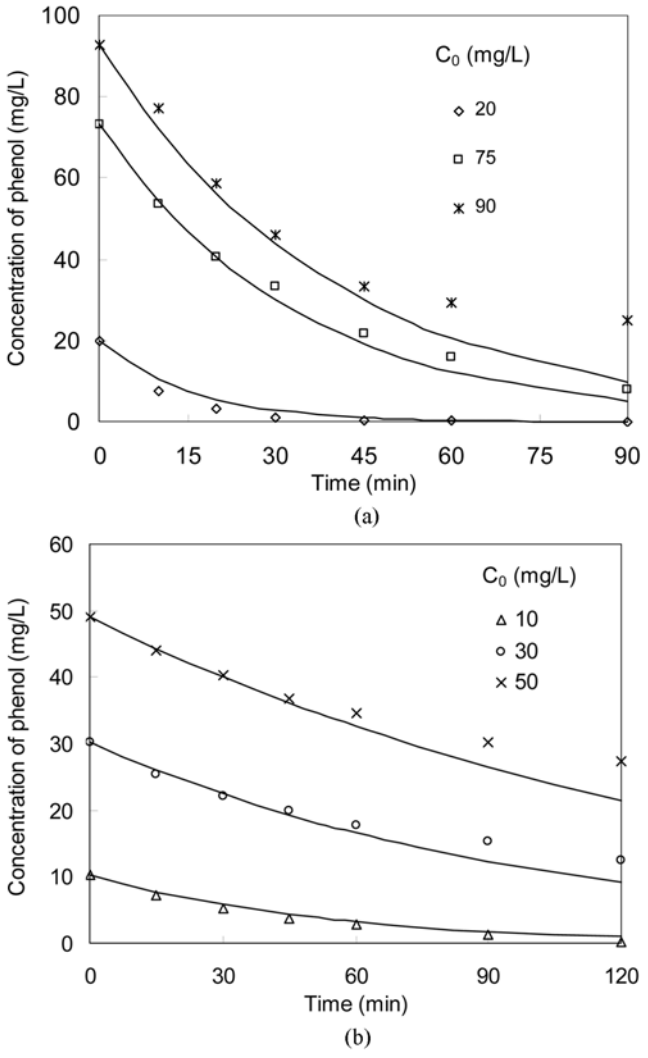

Fig. 13. (a) Langmuir-Hinshelwood kinetics fit for the temporal kinetics of 125 W, aeration, 0.1 g/L TiO_2 (continuous curves are obtained from model values). (b) Langmuir-Hinshelwood kinetics fit for the temporal kinetics of 6 W, 100 L/min aeration, 0.5 g/L TiO_2 (continuous curves are obtained from model values).

the variation of k and K with light intensity. The light intensity (I) effects on the apparent kinetic constant (k) and the apparent adsorption equilibrium constant (K) were represented by the following equations.

$$k = k' I^n \tag{13}$$

and

$$K = \frac{k_a}{k_d + k' I_n} \tag{14}$$

where k_a, k_d, and k are rate constants of the following reactions representing the photocatalysis.

$$A(aq) \underset{k_d}{\overset{k_a}{\rightleftharpoons}} A(ads) \tag{15}$$

$$A(ads) \xrightarrow{k} B \tag{16}$$

In these equations, A refers to the pollutant and B refers to the products of photo degradation.

The L-H constants were also obtained at catalyst loadings other than the optimum ones. The apparent adsorption equilibrium constant K was not found to be sensitive to catalyst loading at higher light intensities. At lower light intensities, the K value did not vary with catalyst loading in a systematic manner. However, the apparent kinetic constant k was found to vary in the same manner as the initial reaction rate. In other words, the apparent kinetic constant k was highest at the optimal catalyst loading.

The effects of various parameters were also compared in terms of quantum yields. The overall quantum yield has been defined as the ratio of initial rate of reaction to the rate of absorption of photons [30]. The quantum yields are lower at high light intensities, because of rate limitation caused by electron-hole recombination reaction [20].

7. Intermediates-quantification

Hydroquinone, catechol, p-benzoquinone, and resorcinol were identified to be the major intermediates at both light intensities. These

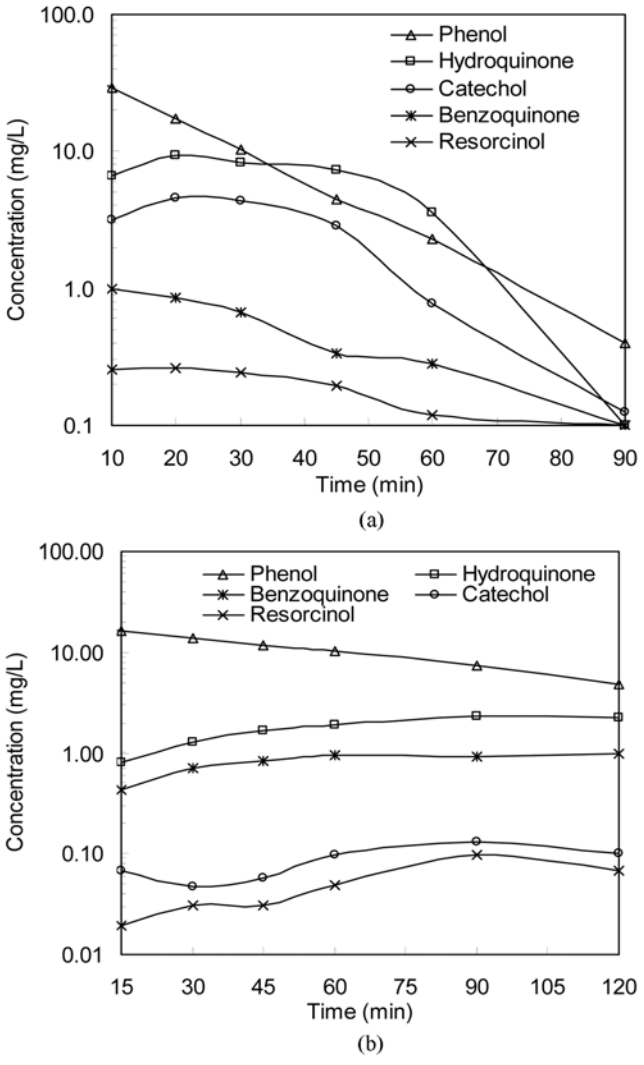

Fig. 14. (a) Intermediates formed during phenol degradation (125 W lamp, aeration, 0.1 g/L TiO_2). (b) Intermediates formed during phenol degradation (6 W lamp, aeration, 0.5 g/L TiO_2).

are similar to the results of Sobczynski et al. [28]. Of these intermediates, hydroquinone was formed the most followed by the other compounds. The intermediates obtained at the respective optimal catalyst loadings at the two light intensities are shown in Fig. 14. Intermediates were quantified by analyzing the chromatogram at the characteristic maximum wavelengths (λ_{max}) of the individual compounds [31]. At the end of reaction, the peaks corresponding to the intermediates could no longer be observed, which indicates their conversion to carbon dioxide and water. The reaction solution was found to have a pink color whenever the mineralization of the feed was not complete. If it were complete, the solution had the color as that of the feed. Sun and Smirniotis [32] and Zhang et al. [33] observed such color changes as well. Sun and Smirniotis [32] attributed it to the possible formation of a rose semiquinone complex from hydroquinone and p-benzoquinone.

For air addition at 125 W (strategy B), the maximum levels of intermediates obtained (expressed as percentage ratio of their concentration relative to the initial phenol concentration) are: hydroquinone (19%), catechol (10%), p-benzoquinone (2%) and resorcinol (0.6%). For air addition at 6 W, hydrquinone (12%) and p-benzoquinone (5%) are found as major compounds followed by catechol (0.7%) and resorcinol (0.5%). From these, it may be seen that the pattern of intermediate formation and degradation is sensitive to light intensity. At low light intensity, more p-benzoquinone was formed in comparison with catechol unlike the trend shown in the higher light intensity case. Similar trends were also observed in the presence of oxygenation.

CONCLUSIONS

From the present study it is concluded that continuous oxygen supply, either in the form of aeration or oxygenation, is essential to sustain the photocatalytic reaction. This is especially valid in closed reactor configurations where uptake of oxygen from the ambient is not possible. Even the strategy of initial pre-saturation of the feed with oxygen without subsequent aeration/oxygenation was observed to sustain the reaction for a limited duration only. The need for oxygen is felt more at high light intensities where more holes and electrons are generated. If the electrons are not scavenged, then the subsequent electron-hole combination prevents further photocatalytic degradation. Further, at high light intensities, the oxygen limitation is a more critical inhibiting factor than the screening effect induced by catalyst loading. Light transmittance measurements may only set an approximate criterion on the required catalyst loading. The dissolved oxygen levels must also be taken into account for evaluating the catalyst loading necessary for optimal reaction rates. With aeration, the optimal catalyst loading was only 0.1 g/L. However, when oxygenation was used, the optimal catalyst loading was actually found increase to 0.25 g/L. At low light intensity, both aeration and oxygenation led to approximately the same optimal catalyst loadings, as it is the light intensity rather than dissolved oxygen concentration that is the limiting factor. Langmuir-Hinshelwood kinetics could be used to predict reasonably the temporal kinetics of phenol photodegradation. L-H constants were found to vary with light intensity and dissolved oxygen concentration in accordance with Ollis [29]. The relative amounts of intermediates formed during phenol degradation were found to depend on the light intensity.

REFERENCES

1. R. Thiruvenkatachari, S. Vigneswaran and I. S. Moon, *Korean J. Chem. Eng.*, **25**, 64 (2008).
2. V. Augugliaro, L. Palmisano, M. Schiavello and A. Sclafani, *Appl. Catal.*, **69**, 323 (1991).
3. E. Pelizzetti and C. Minero, *Electrochim. Acta*, **38**, 47 (1993).
4. L. Devydov, R. Tsekov and P. G. Smirniotis, *Chem. Eng. Sci.*, **56**, 4837 (2001).
5. J. Peral, J. Casado and J. Domenech, *J. Photochem. Photobiol.*, *A*, **44**, 209 (1988).
6. R. Terzian and N. Serpone, *J. Photochem. Photobiol.*, *A*, **89**, 163 (1995).
7. I. Ilisz, Z. Laszlo and A. Dombi, *Appl. Catal.*, *A*, **180**, 25 (1999).
8. C. B. Almquist and P. Biswas, *Chem. Eng. Sci.*, **56**, 3421 (2001).
9. C. Wang, A. Heller and H. Gerischer, *J. Am. Chem. Soc.*, **114**, 5230 (1992).
10. U. Stafford, K. A. Gray and P. V. Kamat, *J. Catal.*, **167**, 25 (1997).
11. T. Hirakawa, T. Daimon, M. Kitazawa, N. Ohguri, C. Koga, N. Negishi, S. Kitazawa and Y. Nosaka, *J. Phochem. Photobiol.*, *A*, **190**, 58 (2007).
12. J.-M. Herrmann, C. Guillard and P. Pichat, *Catal. Today*, **17**, 7 (1993).
13. D. Chen and A. K. Ray, *Appl. Catal.*, *B*, **23**, 143 (1999).
14. I. Kim, H. Ha, S. Lee and J. Lee, *Korean J. Chem. Eng.*, **22**, 382 (2005).
15. M. Salaices, B. Serrano and H. I. de Lasa, *Chem. Eng. Sci.*, **59**, 3 (2004).
16. S. Bekkouche, M. Bouhelassa, N. H. Salah and F. Z. Meghlaoui, *Desalination*, **166**, 355 (2004).
17. D. Curco, S. Malato, J. Blanco, J. Gimenez and P. Marco, *Solar Energy*, **56**, 387 (1996).
18. L. S. Clescerl, A. E. Greenberg and A. D. Eaton, Eds., *Standard methods for the examination of water and wastewater 18th edition*, APHA-AWWA-WEF (1992).
19. C. G. Hatchard and C. A. Parker, *Proc. R. Soc. A*, **235**, 518 (1956).
20. H. Gerischer, *Electrochim. Acta*, **40**, 1277 (1995).
21. R. W. Matthews, *Water Res.*, **24**, 653 (1990).
22. V. Brezova and A. Stasko, *J. Catal.*, **147**, 156 (1994).
23. K. Okamoto, Y. Yamamoto, H. Tanaka and A. Itaya, *Bull. Chem. Soc. Jpn.*, **58**, 2023 (1985).
24. C. S. Turchi and D. F. Ollis, *J. Catal.*, **119**, 483 (1989).
25. K. Chhor, J. F. Bocquet and C. Colbeau-Justin, *Mater. Chem. Phys.*, **86**, 123 (2004).
26. A. V. Emeline, V. Ryabchuk and N. Serpone, *J. Photochem. Photobiol.*, *A*, **133**, 89 (2000).
27. Y. Xu and C. H. Langford, *J. Photochem. Photobiol.*, *A*, **133**, 67 (2000).
28. A. Sobczynski, L. Duczmal and W. Zmudzinski, *J. Mol. Catal.*, *A*, **213**, 225 (2004).
29. D. F. Ollis, *J. Phys. Chem. B.*, **109**, 2439 (2005).
30. N. Serpone, *J. Photochem. Photobiol.*, *A*, **104**, 1 (1997).
31. M. C. Bosco, M. Garrido and M. S. Larrechi, *Anal. Chim. Acta*, **559**, 240 (2006).
32. B. Sun and P. G. Smirniotis, *Catal. Today*, **88**, 49 (2003).
33. L. Zhang, T. Kanki, N. Sano and A. Toyoda, *Environ. Monit. Assess.*, **115**, 395 (2006).